ARCHITECTURE CIVIL ENGINEERING ENVIRONMENT
The Silesian University of Technology No. 2/2015

BACKGROUND, RELIABILITY AND APPLIANCE OF THE CRACK WIDTH PREDICTION METHOD ACCORDING TO EN 13084

Piotr NOAKOWSKI [a], Andreas HARLING [b], Łukasz ZDANOWICZ [c*]

[a] Prof.; Exponent, Kanzlerstaße 4, 40472 Düsseldorf, Germany and Faculty of Architecture and Civil Engineering, TU Dortmund University, August-Schmidt-Str. 8, 44227 Dortmund, Germany

[b] MSc Eng.; Exponent, Kanzlerstaße 4, 40472 Düsseldorf, Germany

[c] MSc Eng.; Faculty of Civil Engineering, Cracow University of Technology, Warszawska 24, 31-115 Kraków, Poland
* E-mail address: *lukasz.zdanowicz@outlook.com*

Received: 22.10.2014; Revised: 29.10.2014; Accepted: 20.01.2015

Abstract
Cracks in concrete are inevitable. Fortunately cracking enables the structure to get rid of its moment peaks. The reduction is due to both: redistribution of the load induced moments and cut of the temperature imposed moments. Furthermore cracking becomes completely harmless if the cracks widths are controlled effectively. In this regard a widely accepted method for crack width prediction is presented in this paper.

Streszczenie
Rysy w betonie są nieuniknione. Na szczęście pojawienie się zarysowania pozwala na wyeliminowanie koncentracji momentów zginających. Redukcja ta wynika z dwóch faktów: redystrybucji momentów zginających powstałych na skutek obciążenia oraz eliminacji momentów wywołanych przez temperaturę. Co więcej, zarysowanie staje się zupełnie niegroźne, jeśli można efektywnie kontrolować szerokość rozwarcia rys. W tym kontekście w niniejszym artykule przedstawiono przegląd powszechnie uznanych metod do przewidywania szerokości rozwarcia rys.

Keywords: **Constraint; Crack width; Deformation behaviour; Non-linear analysis.**

1. BACKGROUND

1.1. Threat of Cracks

Most damage in reinforced concrete structures is attributable to wide separation cracks. One of the classical examples for the thread emerging from wide cracks is the tower wind shield weakened by wide separating cracks (Fig. 1). As the crack width limitation was improper the wind shield was furnished with insufficient hoop reinforcement. This led to formation of wide, vertical cracks subdividing the shell into individual almost free standing strips, which during a hurricane couldn't withstand excessive vertical compression and bulged out. So crack width control is not only for esthetics, durability and tightness but also for the structural integrity which is needed to retain the basic static system and to prevent loss of the load bearing capacity.

1.2. Method Acceptance

To prevent problems with cracks, the Continuous Deformation Theory (CDT) [16, 19] was developed, whose closeness to reality and simplicity in use have led to its wide acceptance in research [01, 02, 03, 09, 15, 17, 23, 24], relevant standards [04 to 07, 11, 25, 26] and dimensioning practice [10, 12, 13, 14, 18, 20, 21, 22, 27, 28, 30, 31]. The CDT is used particularly often in planning and assessment of the industrial structures, where extreme actions and stringent requirements are involved. Due to this the crack control method based

on the CDT was accepted in the following standards:

– DIN 1056 Commentary: On Industrial Chimneys, by Nieser & Engel, 1986 [11],
– CICIND Model Code & Commentaries for Concrete Chimneys, Part A: The Shell, August 2001 [04],
– DIN V 1056: Free-standing Stacks, Calculation and Design, Draft March 2006 [05]
– EN 13084-2: Free-standing Chimneys, Part 2: Concrete Chimneys, January 2006 [07].

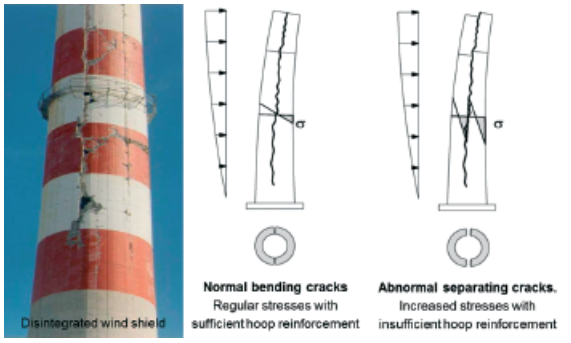

Figure 1.
Threat of cracks – loss of strength as a consequence of wide separating cracks

2. METHOD

2.1. Basic Crack Equation

Crack width w is nothing more than the integral of the steel strains ε within the transfer length a in which the steel bar is being displaced as against concrete (Fig. 2). Consequently, by capturing the strain distribution as a triangle, the crack width can be expressed as its surface:

$$w = a \cdot \varepsilon_m , \tag{1}$$

where:

a – transition length needed to induce steel stress into concrete,

ε_m – mean strain within the transition length.

So the values $a(\sigma)$ and $\varepsilon_m(\sigma)$ are needed to determine the crack width. Since both values are functions of steel stress σ, it is obvious that the crack width w depends on σ^2. Realizing that σ depends on M and ρ, both these magnitudes must be determined properly to control the crack width effectively. Simply said the accuracy of the crack width predictions depends on the correctness of the used internal forces M and N.

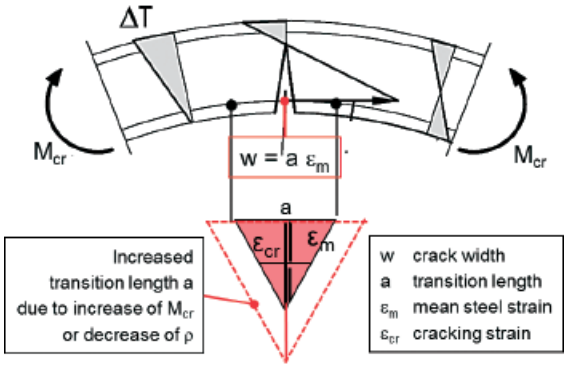

Figure 2.
Basic Crack Equation – from steel strain to crack width

2.2. Crack Propagation

2.2.1. Deformation Behaviour [16, 19]

To understand the nature of the crack control, the polygon like deformation laws (Fig. 3) must be explained by using four individual cracking ranges:

Range 0: No cracks: Primary high stiffness of not cracked component

Range 1: First Crack Formation: Increasing number of individual cracks located far from each other,

Range 2: Final Crack Formation: Final number of numerous cracks with overlapping transition areas

Range 3: Steel Yielding: Plasticization of reinforcement at cracks.

Such polygon like deformation laws provide the following rules:

– The cracking moment is valid for the design:

$$M_{cr} \approx f_{ct} \frac{h^2}{6}, \tag{2}$$

– The cracking temperature ΔT_{cr} is widely independent from the concrete strength f_c:

$$k_T = k_M \quad \Rightarrow \quad \frac{\alpha_T \cdot \Delta T_{cr}}{h} = \frac{2 f_{ct}}{E_c \cdot h} \quad \Rightarrow$$

$$\Rightarrow \quad \Delta T_{cr} = \frac{2 \cdot f_{ct}}{\alpha_T \cdot E_c}, \tag{3}$$

– The steel stress cr depends on the tensile strength of concrete f_{ct}:

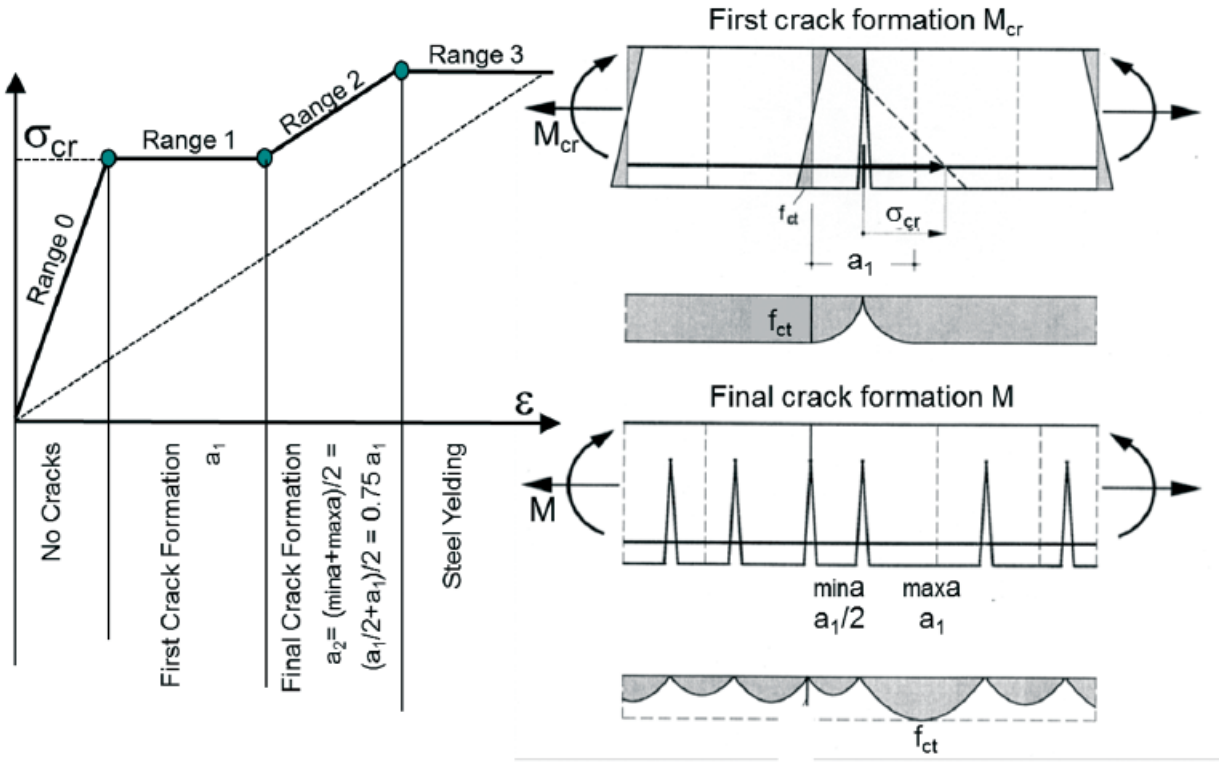

Figure 3.
Crack Propagation – from the first into the final crack formation. Formation of the final crack spacing a_2 out of the transition length a_1

$$M^{I} = M^{II} \quad \Rightarrow \quad \frac{f_{ct} \cdot h^2}{6} \approx \sigma_{cr} \cdot A \cdot 0.8h \quad \Rightarrow$$

$$\Rightarrow \quad \sigma_{cr} \approx \frac{0.2 f_{ct}}{\rho}. \qquad (4)$$

2.2.2. First Crack Formation [16, 19]

The first cracks occur when the bending moment M activated by the temperature difference ΔT reaches its cracking value M_{cr} (Fig. 3). Further increase of ΔT leads only to further cracks without change of M_{cr}. The individual cracks, located far apart from each other, are having invisible transition lengths of a_1 in which the steel bar is displaced against concrete. The entire behaviour with increasing temperature difference ΔT is as follows:

Bending moment	M_{cr}	constant,
Transition length	a_1	constant,
Steel stress	σ_{cr}	constant,
Crack width	w	constant,
Crack number	n_{cr}	increasing.

2.2.3. Final Crack Formation [16, 19]

The final crack occurs when the bending moment M activated by external loads excels the cracking value M_{cr} (Fig. 3). This produces the final stable number of cracks whose visible spacing overlaps and varies between $a_1/2$ and a_1. The crack propagation results in the mean spacing of $a_2 = (a_1/2 + a_1)/2 = 0.75a_1$. The behaviour with increasing moment M is as follows:

Bending moment	M	increasing,
Transition length	a_2	constant,
Steel stress	σ	increasing,
Crack width	w	increasing,
Crack number	n_{cr}	constant.

2.2.4. Realization

In this sense, there is a continuous transformation from the first into the final crack formation. The Continuous Deformation Theory (CDT) takes its name from this phenomenon. The process can be described thoroughly by knowledge of the transition length a_1 within the first crack formation. The value

a_1 obeys the material properties tensile strength of concrete f_{ct} and bond law $\tau = f(\delta)$ defining the bond behaviour between steel and concrete.

2.3. Major relations [16, 19]

2.3.1. Transition Length a_1

The transition length a is the section of the reinforcing bar at the crack in which the steel moves against concrete. Within this section the high steel stress at the crack is transferred by bond stresses into concrete. The transition length obeys the following equation gained from the equilibrium of the bar section in which bond stress is activated:

$$\Sigma\tau = \Sigma\sigma \quad \Rightarrow \quad 2\tau_m \cdot \pi \cdot d_s \cdot a_1 = \frac{\pi \cdot d_s^{\,2}}{4}\sigma_{cr} \quad \Rightarrow$$

$$\Rightarrow \quad a_1 = \frac{d_s \cdot \sigma_{cr}}{2\tau_m}. \tag{5}$$

The mean bond stress τ_m is needed to determine the transition length a (Fig. 4).

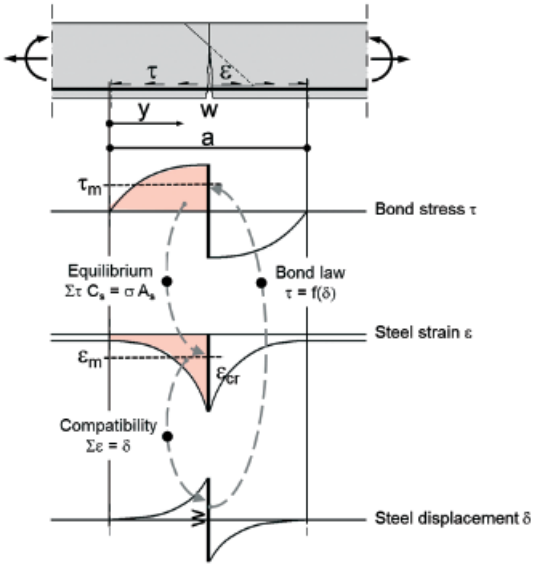

Figure 4.
Major Relations – first crack formation

2.3.2. Bonding Equation

The crucial values within the transition area a_1 are functions of the distance y:

Bond stress $\tau(y)$
Steel strain $\varepsilon(y)$
Steel displacement $\delta(y)$

These functions can be identified by the use of the following links:

Equilibrium

$$\varepsilon_s(y) = \frac{4}{d_s \cdot E_s}\int_0^y \tau(y)dy\,,$$

Compatibility

$$\delta(y) = \int_0^y \varepsilon_s(y)dy = \frac{4}{d_s \cdot E_s}\int_0^y\int_0^y \tau(y)dy\,dy\,,$$

Bond law

$$\delta(y) = \left(\frac{\tau(y)}{A \cdot f_{cm}^{\frac{2}{3}}}\right)^{\frac{1}{N}},$$ where A and N bond laws factors.

By equalizing the displacements the following bonding equation is gained:

$$\left(\frac{\tau(y)}{A \cdot f_{cm}^{\frac{2}{3}}}\right)^{\frac{1}{N}} = \frac{4}{d_s \cdot E_s}\int_0^y\int_0^y \tau(y)dy\,dy\,. \tag{6}$$

2.3.3. Crucial Magnitudes

The resolution in terms of the bond stress distribution $\tau(y)$ provides the following crucial magnitudes:

– Mean bond stress within the transition area:

$$\tau_m = \left(\frac{2^{-3N}(1-N)^{(1+N)}}{1+N}\frac{A}{E_s^{\,N}} f_{cm}^{\,0.66} \cdot d_s^{\,N} \cdot \sigma_{cr}^{\,2N}\right)^{\frac{1}{1+N}}, \tag{7}$$

– Mean steel strain within the transition area:

$$\varepsilon_m = \frac{1-N}{2}\varepsilon_{cr}\,, \tag{8}$$

– The expressions can be simplified by insertion of the bond law values $A = 0.95$ and $N = 0.12$:

$$\tau_m = \left(0.13 f_{cm}^{\,0.66} \cdot d_s^{\,0.12} \cdot \sigma_{cr}^{\,0.24}\right)^{0.89}, \tag{9}$$

$$\varepsilon_m = 0.44\varepsilon_{cr}, \tag{10}$$

– The equilibrium of the stresses acting on the bar provides the transition length:

$$a_1 = \frac{d_s \cdot \sigma_{cr}}{2\tau_m}. \tag{11}$$

2.4. Full Crack Equation [16, 19]

2.4.1. Design Equation

By use of the above crucial magnitudes and by introduction of the crack development factor C_E the following full crack equation was found:

$$w_k = \gamma_w \cdot C_E \cdot a_1 \frac{(\sigma_s - C_E \cdot 0.56\sigma_{cr})}{E_s}, \tag{12}$$

where:

$wk = \gamma_w \cdot w_m$	characteristic crack width [mm],
$\gamma_w = 1.50$	dispersion factor,
$C_E = 1.00$ at $\sigma_s = \sigma_{cr}$	crack development factor, first crack formation,
$C_E = 0.75$ at $\sigma_s > \sigma_{cr}$	crack development factor, final crack formation,
$a_1 = \sigma_{cr}/\tau_m \cdot d_s/2$	crack transition length [mm],
$\sigma_{cr}(M_{cr}, N_{cr})$	crack stress depending on f_{ct} and the cross sectional values [MPa],
$\sigma_s(M, N)$	acting stress depending on M, N and the cross sectional values [MPa],
$\tau_m = (0.13 \cdot f_{cm}^{0.66} \cdot d_s^{0.12} \cdot \sigma_{cr}^{0.24})^{0.89}$	mean bond stress for deformed bars [MPa],
f_{ct}	tensile concrete strength [MPa],
E_s	E-Modulus for reinforcement [MPa],
d_s	bar diameter [mm],
$\rho = A_s/(bh)$	ratio of reinforcement.

2.4.2. Method Efficiency

The method covers the following 15 influences in total:

Tensile strength f_{ct}:	concrete strength f_{cm}, predamage, eccentricity, thickness,
Bond law τ:	concrete strength f_{cm}, bar profilation a_R, bonding position, concrete cover c/d_s,
Actions:	internal forces M and N, temperature,
Reinforcement:	ratio ρ, bar diameter d_s,
Crack range:	first and final crack formation.

The continuous crack equation can be adapted for any sort of concrete and steel and for any load actions. Because of this, the method is generally used in the field of theoretical research and in practice.

2.5. Standard Crack Equation [04, 05, 07, 25]

2.5.1. Design Equation

In the standards EN 13084, CICIND Model Code and DIN 1056 (Fig. 5) the following simplified equation is used:

$$w_k = 3.5\left(\frac{\sigma_{cr}^{0.88} \cdot d_s}{f_{cm}^{0.66}}\right)^{0.89} \frac{\sigma_s - 0.4\sigma_{cr}}{E_s}. \tag{13}$$

In the case of the most important first crack formation with acting stress σ_s equals the cracking stress σ_{cr}, the equation becomes even more transparent:

$$w_k = 2.1\left(\frac{\sigma_{cr}^{2.00} \cdot d_s}{f_{cm}^{0.66}}\right)^{0.89} \frac{1}{E_s},$$

$$\sigma_{cr} = \frac{M_{cr}}{W_{II}} = f_{ct}\frac{W_I}{W_{II}} \approx f_{ct}\frac{h^2}{6}(A_s \cdot 0.8h) = 0.21\frac{f_{ct}}{\rho}$$

(estimation),

$M_{cr} = f_{ct} W_I$ [MNm],

$$f_{ct} = \frac{0.35(0.85 - 0.2h)(2.6 + 24h)}{1.0 + 40h} f_{cm}^{\frac{2}{3}}$$

(pure bending),

$f_{cm} = f_c + 8$ [MPa],

h [m]

$\rho = A_s/A_c$,

d_s [mm],

$E_s = 210\,000$ [MPa].

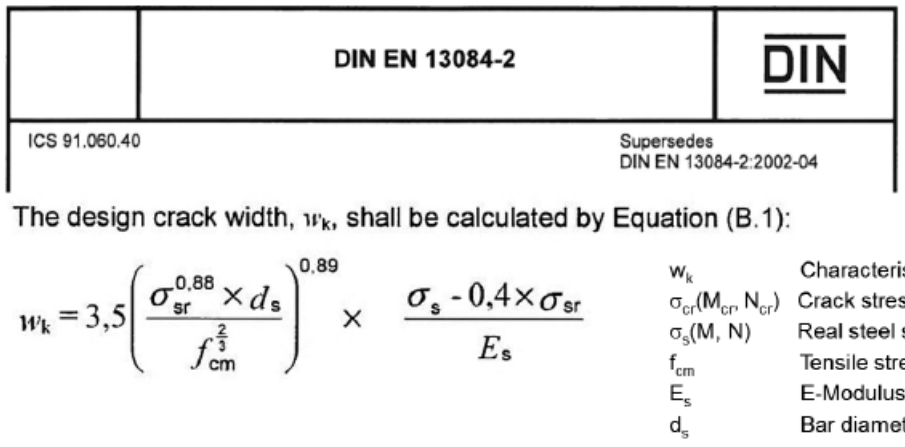

Figure 5.
Crack Equation – mandatory in EN 13084, CICIND Model Code, DIN 1056

2.5.2. Design Process

The process of the crack control involves the following data collectives:

– Input Data — Steel and concrete properties, dimensions, loads, temperature,
– Design Criteria — Steel stress $\sigma_s < f_y$, crack width $w_k < w_{lim}$, bar spacing $s_{min} < s < s_{max}$,
– Output Data — Thickness h, ratios of reinforcement ρ, bar diameters d_s.

Since such process is not very transparent and requires some effort, appropriate Design Charts are offered in the Design Manual [25].

3. RELIABILITY

3.1. Measurements vs Predictions [15, 29]

The aim of the laboratory tests on beams was to gain information about the general crack behaviour. The used specimens were as follows:

Concrete strengths — f_{cm} = 13 to 23 MPa,
Reinforcement levels — ρ = 0.42 to 0.86%,
Bar diameter — d_s = 10 to 26 mm,
Bar positions — h_1 = 27 to 66 mm,
Steel stresses — s = 150 to 400 MPa.

Within the valuations in the corresponding crack widths w_k were calculated [15] by means of the steel stresses σ_s determined in accordance with the notified loads and beam characteristics. The comparison between the measured and the calculated crack widths w_k confirms the realistic nature of the prediction by the presented method from EN 13084. This is expressed in the relatively small scatter of only 15% around the ideal line (Fig. 6).

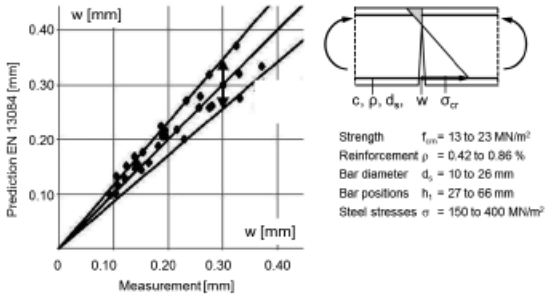

Figure 6.
Experimental Measurements vs Analytical Predictions

3.2. Impact of Concrete Cover [08, 25]

The aim of the computation study regarding cracks in beams was to gain clues about the following issues:

– Impact of the features f_c, h, c, ρ and d_s on the behavioural features steel stress σ_s and crack width w,
– Comparison of the computation results predicted by EN13084 [07] and by EC2 [08].

The numerous considered beam variants were as follows in Fig. 7.

The results of the study regarding the impact of the concrete cover c allow the following statements regarding the agreement between EN 13084 and EC2:

σ_s — relatively good agreement,
w_k — poor agreement in the range c < 30 mm where EC2 behaves incomprehensibly discontinuous.

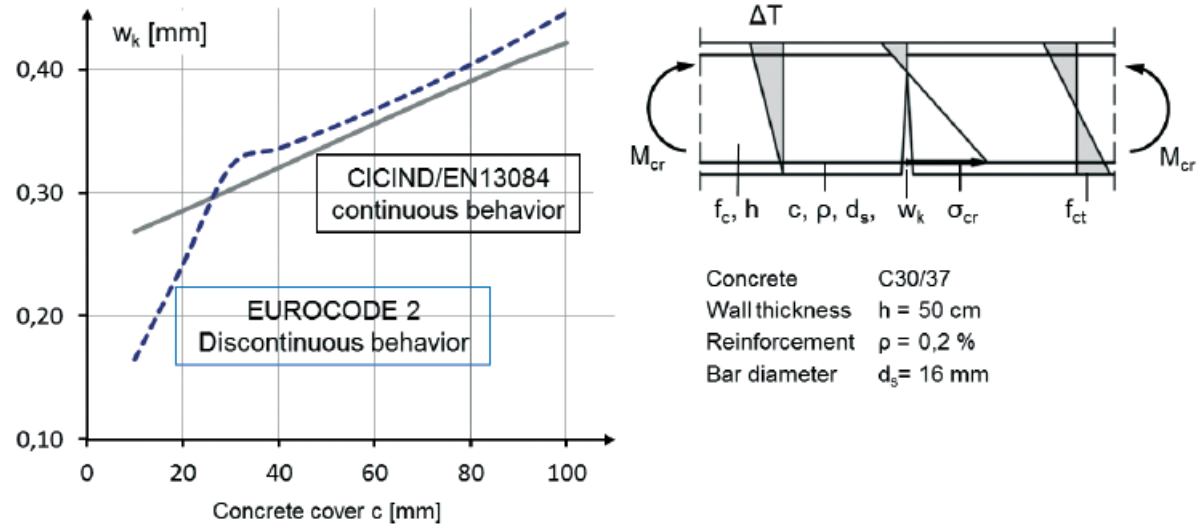

Figure 7.
Impact of concrete cover *c* on crack width

4. APPLIANCE

4.1. Leaking Foundation Slab [27]

Numerous cracks with water spills appeared alongside the border of a large foundation slab (Fig. 8). The damage was caused by a severe slab cooling in the wintertime which activated tension and so produced separating cracks. The general slab features and the load actions are as follows:

Concrete	C30/37 WU,
Steel	S500,
Coating	OS-8,
Thickness	h = 1.0 m,
Reinforcement	d_s = 20 mm, s = 12 cm, c = 4.5 cm,
Water pressure	p = 40 kN/m²,
Shrinkage	ε_s = -0.05‰ (-5K) (uniform),
Temperature	ΔT_G = +5K to -10K (difference),
	ΔT_M = -5K + ΔT_G/2 (uniform drop).

The crack behaviour identified by measurements, drilling cores and microscopic photos are as follows:

Total crack length	500 m, yearly increase by 100 m,
Crack length with spills	100 m,
Cracks crossing aggregate	⇒ formation after concrete hardening,
Normal cracks in concrete < 0.4 mm	⇒ elastic steel behaviour,
Wide cracks in coating > 0.4 mm	⇒ delamination and erosion at the crack edges.

4.2. Leakage Explanation [27]

The leakage was caused by excessive crack widths which enabled the ground water to intrude into the building. The committed mistakes consisted in non-critical designing of the slab by EC2. Their explanation by comparing with the design by EN13084 is as follows (Fig. 9).

4.2.1. Incorrect Crack Prediction by EC2

- Selection of the initial ratio of reinforcement of ρ = 0.26 %,
- Assumption of the crack formation at early concrete age with a low tensile strength f_{ct} = 1.5 MPa,
- Further reduction of the tensile strength by factor 0.5 through postulating distinct own stresses,
- Underestimation of the cracking stress in the reinforcement σ_s = 143 MPa,
- Severe underestimation of the crack width w_k = 0.20 mm due to the dependency $w(\sigma_s^2)$,
- Acceptance of the initially selected ratio of reinforcement of ρ = 0.26 % as sufficient.

4.2.2. Correct Crack Prediction by EN 13084

- Selection of the initial ratio of reinforcement of ρ = 0.26 %,
- Assumption of the crack formation at mature concrete age with a high tensile strength f_{ct} = 2.1 MPa,
- No reduction of the tensile strength by own stresses,

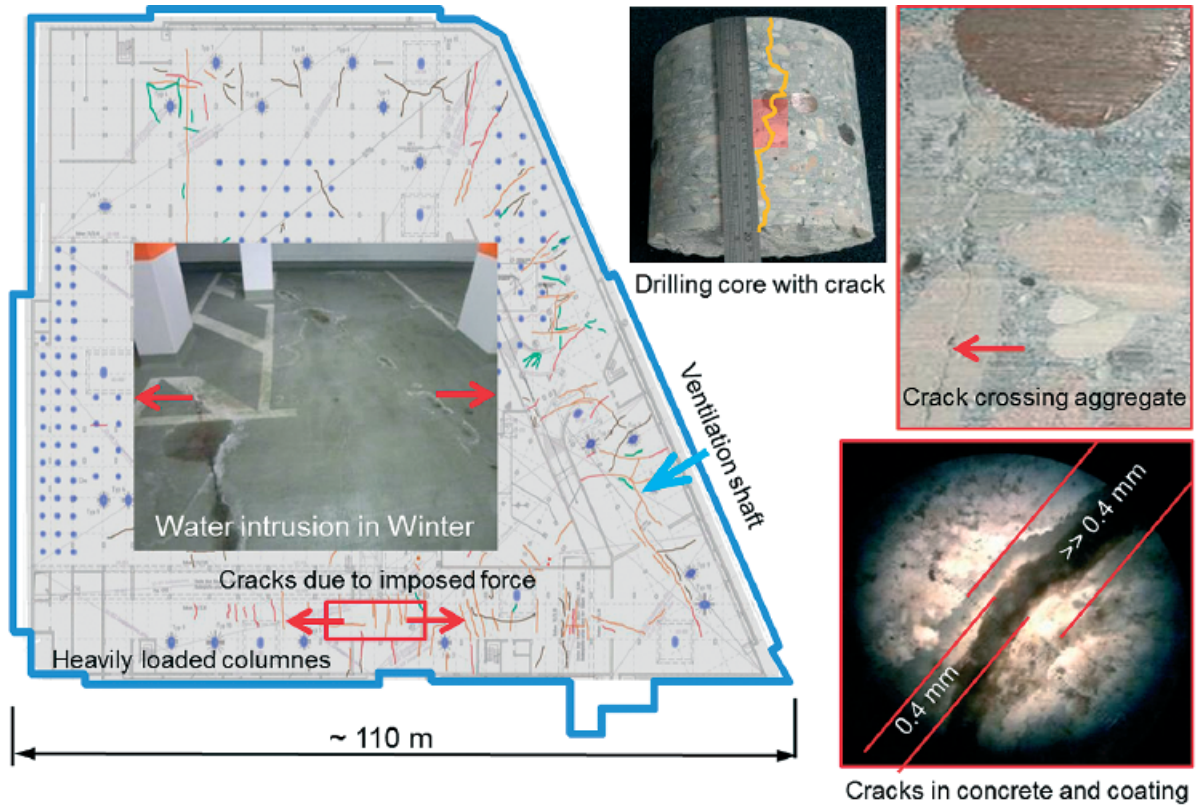

Figure 8.
Leaking Foundation Slab – loss of tightness due to wide through cracks

– Correct estimation of the cracking stress in the reinforcement $\sigma_s = 419$ MPa,
– Correct estimation of the crack width $w_k = 0.78$ mm due to the dependency $w(\sigma_s^2)$,
– Rejection of the initially selected ratio of reinforcement of $\rho = 0.26$ % as insufficient.

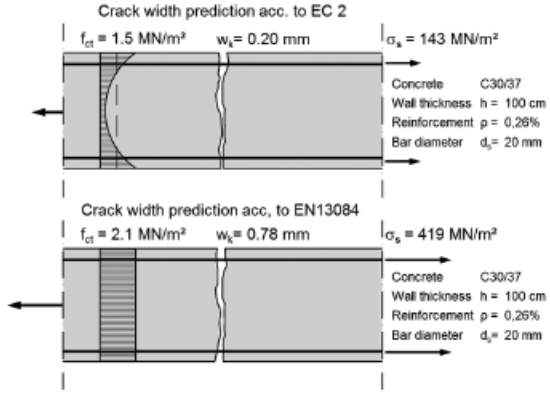

Figure 9.
Leakage Explanation – crack width prediction according to EC2 and EN 13084

5. FINAL REMARKS

The crack prediction method in EN 13084 deserves the following ratings:

– Physical Purity: *Fulfilment of all mechanical rules incl. the non-linear structure behaviour*,
– Simplicity in Use: P*resence of one transparent equation for all designing scenarios*,
– Universality in Appliance: *Validity for all crack formation ranges, any reinforcement, any eccentricities*,
– Closeness to Reality: *Agreement with test results and experiences*,
– Wide Acceptance: *Entry into several standards and general use in research and practice*.

The corresponding seven key features of the method in EN 13084 are as follows:

(1) Consistent with the Continuous Deformation Theory (CDT),
(2) Satisfying the rules of equilibrium, compatibility and material laws ,
(3) Applicable to any bond and tensile strength conditions,

(4) Valid for any ranges of crack formation (first & final) and for extreme reinforcement ratios,

(5) Valid for temperature and load action as well as for any eccentricity M/N,

(6) Continuous to all parameters,

(7) Suitable for stochastic analysis.

ACKNOWLEDGMENTS

The paper was presented at the 8th International Conference AMCM 2014 – Analytical Models and New Concepts in Concrete and Masonry Structures (AMCM'2014), Wrocław, June 2014.

REFERENCES

[1] *Bierrum N. R. et al.*; The revised CICIND Model Code for Concrete Chimneys. CICIND Report, Vol.14, No. 2, 1999; p.121-129

[2] *Bottenbruch H., Noakowski P.*; Versagens-wahrscheinlichkeit von turmartigen Bauwerken (Failure Probability of Tower-Like Structures). Bauingenieur, Vol.62, No.1, 1987; p.29-40 (in German)

[3] *Bruggeling A. S. .G.*; Structural Concrete, Theory and its Application; Balkema; Rotterdam, Netherlands, 1991

[4] CICIND: Model Code and Commentaries for Concrete Chimneys. Part A: The Shell. CICIND, 1984 & 2001

[5] DIN V 1056: Freistehende Schornsteine in Massivbauart, Berechnung und Ausführung (Free Standing Chimneys as Solid Structures). Deutsches Institut für Normung e. V., Ersatz für DIN 1056; Entwurf, 2005 (in German)

[6] DVGW; Planung und Bau von Wasserbehältern (Design and Construction of Water Tanks); Deutscher Verein für Gas- und Wasserwirtschaft. Technische Regeln, Arbeitsblatt W311; 1988 (in German)

[7] EN 13084: Freistehende Schornsteine, Teil 2: Betonschornsteine (Free-standings chimneys – Part 2: Concrete chimneys). Normenausschuss Bauwesen (NABau) im DIN e.V., 2002 (in German)

[8] EN 1992-1-1:2004 + AC:2008; Eurocode 2: Design of concrete structures – Part 1-1: General rules and rules for buildings. European Committee For Standardization, 2004/2008

[9] *Frank K., Litzenburger M., Peters G.*; Rissnachweis nach Noakowski aufbereitet für den Taschenrechner (Crack control according to Noakowski adopted for pocket calculators). Bautechnik, Vol.65, No.5, 1988; p.174-177 (in German)

[10] *Lohmayer G., Ebeling K.*; Weiße Wannen – einfach und sicher (White tub – simply and without fail). Verlag Bau + Technik, Düsseldorf, Germany, 2009 (in German)

[11] *Nieser, H., Engel V.*; Industrieschornsteine in Massivbauart, Kommentar zu DIN 1056 (Industrial chimneys in construction of concrete structures). Beuth, Berlin, Germany 1986 (in German)

[12] *Noakowski P, Gerstle K.*; Tower Structures Subjected to Temperature and Wind. ACI Structural Journal, Vol.97, No.4, 1990; p.479-489

[13] *Noakowski P., Baumann T., Topp T., Aigner, F.*; Vorgespannte Flüssiggas-Behälter (Prestressed tank for liquid gas). Bauinformatik, No.6, 1991; p.10-20 (in German)

[14] *Noakowski P., Keuser M., Brunssen G., Günther, H.*; Stahlbetontunnel (Reinforced Concrete Tunnel). Bauinformatik, No.3, 1992; p.20-30 (in German)

[15] *Noakowski P., Bierrum R., Schäfer A. G., Woitzik M.*; Control of Crack Width. CICIND Report, Vol.15, No.2; Salzburg, France, 1999

[16] *Noakowski P., Schäfer H.G.*; Steifigkeitsorientierte Statik im Stahlbetonbau (Stiffness Oriented Design of Reinforced Concrete Structures). Ernst & Sohn, Berlin, Germany, 2003 (in Germany)

[17] *Noakowski P., Breddermann M., Harling A., Schnetgöke J.*; Rissbildung in turmartigen Tragwerken, Schleuderbetonmast vs. Stahlbeton-schornstein (Crack Formation in Tower like Structures: Mast of Centrifugal Concrete vs. Chimney of Normal Concrete). Beton- und Stahlbetonbau, Vol.100, No.7, 2005; p.538-548 (in German)

[18] *Noakowski P., Breddermann M., Harling A., Rost M.*; Strengthening of Tower-Like Structures. CICIND Chimney Book, The International Chimney Association CICIND, Ratingen, Germany, 2006

[19] *Noakowski P., Breddermann M., Harling A., Rost M.*; Turmartige Industriebauwerke, Grundlagen der CICIND, DIN EN 13084 (Industrial Tower Structures – Basics of CICIND, DIN EN 13084). Betonkalender 2006, Part 1, p.223-318 (in German)

[20] *Noakowski P., Leszinsk, H., Breddermann M., Rost M.*; Schlanke Hochbaudecken. Steifigkeitsorientierte Analyse zur Klärung extremer Durchbiegungen (Slender Building Floors, Clarification of Extreme Deflections). Beton- und Stahlbetonbau, Vol.103, No.1, 2008; p.28-37 (in German)

[21] *Noakowski P., Harling A., Breddermann M., Rost, M.*; Windkraftwerke – Umwelt, Bemessung, Perspektiven (Wind Turbine – Environment, Design, Perspectives). Bautechnik, Vol.86, No.9, 2009; p.574-585 (in German)

[22] *Noakowski P., Breddermann M., Harling A., Rost M., Potratz S., Leszinski H.*; Verstärkung turmartiger Bauwerke (Strengthening of Tower Structures)

Beton- und Stahlbetonbau, Sonderheft „Kraftwerksbau“, Vol.98, No.10, 2003; p.583-595 (in German)

[23] *Noakowski P.*; Close to Reality Methods for the Structural Design of Towers. The basics of the Relevant Standards for Industrial Chimneys. Architecture – Civil Engineering – Environment, Vol.3, No.3, 2010; p.79-84

[24] *Noakowski P.*; Proper Design of the RC Structures in Terms of Use of the Realistic Moments. In Proc. Central European Congress on Concrete Engineering, Wroclaw, Poland, 2013; p.432-440

[25] *Noakowski P.; M., Harling A., Rost M.*; Manual for the Design of Concrete Chimneys (Draft). CICIND Autumn Meeting, Paris, France, 2013; p.123-131

[26] *Noakowski P., Moncarz P.*; Eurocode EN 13084 Approach on Crack Width Prediction. ACI Spring Convention, Reno, USA, 2014

[27] *Noakowski P., M., Harling A., Michalak B.*; Szczelność płyty fundamentowej pod maszynownią (Leakproofness of foundation slab for engine room). In Proc. ENERGIA 2014, Karpacz, Poland, 2014; p.234-242 (in Polish)

[28] *Pfefferkorn W., Steinhilber H.*; Ausgedehnte fugenlose Stahlbetonbauten (Long Reinforced Concrete Constructions without Dialtations). Beton-Verlag, Berlin, Germany, 1990 (in German)

[29] *Rüsch H., Rehm G.*; Versuche mit Betonformstählen (Experiments of Reinforcement Steel). Deutscher Ausschuss für Stahlbeton, No.140/160, Berlin, Germany, 1963/1966 (in German)

[30] *Schnell J., Kautsch R., Noakowski P., Breddermann M.*; Verhalten von Hochbaudecken bei Zugkräften aus Zwang (Behaviour of Building Floors with Imposed Longitudinal Forces). Beton- und Stahlbetonbau, Vol.100, No.5, 2005; p.406-415 (in German)

[31] VGB PowerTech, Industrieschornsteine, Hinweise zur Bauausführung und Inbetriebnahme Merkblatt (Industrial Chimneys – Evaluation of the Construction Methods, Notes on Design and Commissioning), VGB-M 642 U, Essen, Germany, 2003